Positive Feedback in the AKT/mTOR pathway and its implications for growth signal progression in skeletal muscle cells: An analytical study

Fernando López–Caamal[a], Míriam R. García[a], Richard H. Middleton[a], Heinrich J. Huber[b,*]

[a] *Hamilton Institute, National University of Ireland, Maynooth, Co. Kildare, Ireland.*
[b] *Centre of Systems Medicine, Department of Physiology & Medical Physics, Royal College of Surgeons in Ireland, Dublin, Ireland.*

Abstract

The IGF-1 mediated AKT/mTOR pathway has been recently proposed as mediator of skeletal muscle growth and a positive feedback between Akt and mTOR was suggested to induce homogenous growth signals along the whole spatial extension of such long cells. Here we develop two biologically justified approximations which we study under the presence of four different initial conditions that describe different paradigms of IGF-1 receptor–induced Akt/mTOR activation. In first scenario the activation of the feedback cascade was assumed to be mild or protein turnover considered to be high. In turn, in the second scenario the transcriptional regulation was assumed to maintain defined levels of inactive pro–enzymes. For both scenarios, we were able to obtain closed–form formulas for growth signal progression in time and space and found that a localised initial signal maintains its Gaussian shape, but gets delocalised and exponentially degraded. Importantly, mathematical treatment of the reaction diffusion system revealed that diffusion filtered out high frequencies of spatially periodic initiator signals suggesting that the muscle cell is robust against fluctuations in spatial receptor expression or activation. However, neither scenario was consistent with the presence of stably travelling signal waves. Our study highlights the role of feedback loops in spatiotemporal signal progression and results can be applied to studies in cell

*Corresponding author. Tel.: + 353 1 402 8538; Fax: + 353 1 402 2447.
Email address: Heinhuber@rcsi.ie (Heinrich J. Huber)

proliferation, cell differentiation and cell death in other spatially extended cells.

Keywords: AKT/mTOR, Skeletal muscle, Positive feedback, Protein activation, PDE, Analytical solutions

---

1. Introduction

The Insulin-like growth factor (IGF-1) receptor pathway is a canonical pathway that mediates cell growth and survival. Upon growth factor binding to the receptor, the lipid kinase phosphoinositide-3-OH kinase (PI3K) gets phosphorylated and activated. This activation leads to phosphorylation and activation of the pro–survival kinase Akt. Through a double inhibitory step, active Akt leads to the activation of the mammalian target of rapamycin (mTOR) which switches on anabolic processes such as protein or nucleotide production. In turn, evidence has been provided that mTOR can phosphorylate and activate Akt [15, 31], thereby establishing a positive feedback loop.

Recent reports suggested the IGF-1 mediated PI3K-/Akt-/mTOR pathway to be a regulator of muscle cell growth. Indeed, studies that overexpressed active AKT by genetic mutations or pharmacological activation reported an increase in muscle fibre diameter (muscular hypertrophy) while muscle fibre diameter decreased upon inhibition of Akt or mTOR (muscular atrophy) [26, 3, 29]. Trophic factor receptors such as IGF-1 can be randomly and anisotropically distributed along the cell surface [14, 17, 35] and activation of Akt by PI3K has been determined to be localised at the receptors. Therefore it remains to be understood how a signal that is associated with certain locations on the surface of a muscle cell can proceed through the entire spatial extension of this cell in a homogenous fashion. Diffusion alone cannot be responsible for eliminating spatial gradients in larger cells as protein motility is limited by ubiquitenation and degradation of activated proteins [16]. It is therefore assumed that the Akt/mTOR positive feedback loop acts as a signal regenerator [9, 21, 33] in larger cells.

In this study, we will investigate a mathematical model that studies Akt/mTOR signal progression in skeletal muscle cells with an anisotropic distribution of IGF-1 receptors on the muscle cell surface. We will focus on an analytical treatment to study whether general principes of the resulting reaction diffusion equation can be derived. We will first discuss the time dependent, spatially invariant reaction system of a simple auto-activation

network of Akt/mTOR and obtain criteria for stable enzyme activation. Subsequently, we will include one spatial dimension, so as to idealize the muscle cell as a linearly extended compartment and focus on two biologically reasonable scenarios that we solve in the presence of four different initiator signals. While no travelling waves are present under these assumptions, we will observe that the feedback loop together with diffusion can filter out spatial anisotropies. This filtering allows the translation of anisotropies arising from an inhomogenous distribution of IGF-receptor or from fluctuations in the initiator signals into a homogenous Akt/mTOR activation along the cell. We will further discuss the implications of our findings on receptor mediated activation in other large cells such as nerve cells.

2. Temporal dynamics of the Akt/mTOR autoactivation network

As we strive to obtain analytical solutions, we keep our system simple and represent it as a motif that is ubiquitously present in signalling pathways (see for example [16]). We concentrate on a time dependent analysis of the positive feedback loop to better characterise the basic feature of our reaction cascade. Instead of investigating a mutual activation between Akt and mTOR, we abstract the entire Akt/mTOR cassette into single node which activates itself. This assumption is justified when mTOR levels vary more slowly than Akt, or the pool of mTOR is abundant in comparison to that of Akt, as shown in Appendix 7.1. We further include a potential inhibitor of this Akt/mTOR node, which could be an Akt pharmacological antagonist, the Akt inhibitor Phospholipid Phosphatase SHIP-2 [34], or the tumour surpressor kinase Protease and tensin homolog (PTEN) [22, 23]. Moreover, we assume that the Akt/mTOR form gets produced as inactive pro–form (P) and gets degraded when it is active (A). Only the active form is assumed to effect downstream signalling [23]. The resulting network is defined by

$$P + A \xrightarrow{k_1} 2A \tag{1a}$$

$$A \xrightarrow{k_2} 0 \tag{1b}$$

$$P \underset{k_{3b}}{\overset{k_{3f}}{\rightleftharpoons}} 0 \tag{1c}$$

$$A + I \xrightarrow{k_4} 0 \tag{1d}$$

$$I \underset{k_{5b}}{\overset{k_{5f}}{\rightleftharpoons}} 0. \tag{1e}$$

Upon the presence of an active form A, the inactive pro–form P gets activated (auto–activation, (1a)). In the kinetics of the auto–activation (1b), k_1 is set proportional to the product of the amount of the active and of the inactive form (consistent with the assumption of mass-action kinetics). The active form is assumed to get degraded (1b) and this degradation rate is assumed to be proportional to its concentration (factor k_2). Protein turnover was modelled to establish the pro–form P and the inhibitor I at constant expression levels (1c) and (1e), respectively. This was achieved by balancing protein production (linear factors k_{3b} and k_{5b} for inactive form and inhibitor) with protein degradation (first order proportionality constants k_{3f} and k_{5f}). Inhibition of the active form is assumed according mass action kinetics (1d).

Defining the vector $\mathbf{c} = (c_1\ c_2\ c_3)^T := ([P]\ [A]\ [I])^T \in \mathbb{R}^3_+$, we obtain the following set of coupled ordinary differential equations (ODE) (see [18], for details)

$$\dot{c}_1 = -k_{3f}c_1 - k_1c_1c_2 + k_{3b} \tag{2a}$$
$$\dot{c}_2 = -k_2c_2 + k_1c_1c_2 - k_4c_2c_3 \tag{2b}$$
$$\dot{c}_3 = -k_{5f}c_3 - k_4c_2c_3 + k_{5b}. \tag{2c}$$

Without the inhibitor, we obtain

$$\dot{c}_1 = -k_{3f}c_1 - k_1c_1c_2 + k_{3b} \tag{3a}$$
$$\dot{c}_2 = -k_2c_2 + k_1c_1c_2. \tag{3b}$$

Due to the nonlinearity of this equation, a straightforward mathematical solution of the temporal dynamics is not possible. However, we can calculate the steady state protein levels for the inactive form ($\bar{c}_1$) and the active form ($\bar{c}_2$) in the auto–activation cascade,

$$\text{off state: } = \{\bar{c}_{1,off}, \bar{c}_{2,off}\} \ = \ \left\{\frac{k_{3b}}{k_{3f}}, 0\right\} \tag{4a}$$
$$\text{on state: } = \{\bar{c}_{1,on}, \bar{c}_{2,on}\} \quad = \ \left\{\frac{k_2}{k_1}, \frac{k_{3b}}{k_2} - \frac{k_{3f}}{k_1}\right\}. \tag{4b}$$

Here, we have denoted the state where no active form is present as the 'off state' while the other state was denoted as 'on state'. We next investigated under what conditions these steady states are stable against small perturbation. Such a local stability analysis has been extensively described by [7].

In brief, local stability requires that the eigenvalues of the Jabocian matrix that were derived from the system (2a)–(2c) have negative real parts. The eigenvalues are roots of the characteristic polynomial

$$P(s) \;=\; s^2 + (k_1\,[\bar{c}_2 - \bar{c}_1] + k_2 + k_{3f})\,s + k_1\,(k_2\bar{c}_2 - k_{3f}\bar{c}_1) + k_2 k_{3f}.$$

The Routh–Hurwitz criterion applied to a second order polynomial, states that the roots of such a polynomial will be negative, when all the coefficients have the same sign. From this criterion, we conclude that the 'off steady state' will be locally stable if and only if $k_1 < k_2\; k_{3f}/k_{3b}$; in turn, for the 'on steady state' to be stable, we require $k_1 > k_2\; k_{3f}/k_{3b}$.

Figure 2(a) depicts the location and stability of the steady states for c_2 as a function of the feedback strength (k_1). While a value less than 0.04 $[(\mu M \text{ min})^{-1}]$ renders the 'off state' stable (solid line), this state becomes unstable (dashed line) for $k_1 > 0.04[(\mu M \text{ min})^{-1}]$. For values above this threshold, the 'on state' becomes positive and stable, therefore biologically meaningful. Similar results can be obtained for analysing the stability of both states in dependence of other kinetic parameters. We conclude that a stable activation is not always present, but requires the condition $k_2/k_1 < k_{3b}/k_{3f}$ to be fulfilled. If the conditions of a stable state are not met, any initial activation will go back to zero over time. Whenever conditions for a stable 'on state' are met, both active and inactive forms will eventually converge to this state (see trajectories, and phase portrait in Figure 2(b–d)). In Figure 2(d), the solid line represents an orbit of the system that converges to the stable steady state. Similarly, the orbit represented by the dotted line, will converge to the stable steady state, even if its initial condition is very close to the unstable steady state. In contrast, the orbit whose initial condition lies in the axis $c_2(t) = 0$ will converge to the unstable steady state. This shows that this unstable steady state is a saddle point.[1] In turn, the stable steady state is a focus.

3. Spatio–temporal dynamics of Akt/mTOR autoactivation

While in the last section we concentrated on the temporal regulation of the auto–activation network and studied the systems under equilibrium

[1] In fact, all the orbits which start in the axis $c_2(t) = 0$, will converge to the unstable steady state since this is the stable manifold of the saddle point.

conditions, we are now interested in the spatial and temporal dynamics of the active form $c_2(t, x)$. We will model the muscle cell as a cell with large spatial extension, therefore neglect its diameter and consider a one dimensional spatiotemporal model. In addition, we assume that IGF receptors are anisotropically distributed along the cell surface where they lead to an initial Akt/mTOR activation. We finally assume that active Akt/mTOR will exercise its effect at each spatial location where it is present.

By including one dimensional diffusion according Fick's laws [2], the equation system (2) transforms into the following set of Partial Differential Equations (PDEs),

$$\frac{\partial}{\partial t}c_1 = d_1\nabla_x^2 c_1 - k_{3f}c_1 - k_1 c_1 c_2 + k_{3b} \tag{5a}$$

$$\frac{\partial}{\partial t}c_2 = d_2\nabla_x^2 c_2 - k_2 c_2 + k_1 c_1 c_2 - k_4 c_2 c_3 \tag{5b}$$

$$\frac{\partial}{\partial t}c_3 = d_3\nabla_x^2 c_3 - k_{5f}c_3 - k_4 c_2 c_3 + k_{5b}, \tag{5c}$$

with the diffusion constants d_1, d_2, d_3 for inactive form, active form and inhibitor.

We first note that the steady states of the space independent scenario (4) are also steady states of the reaction diffusion equation (5). Nevertheless, the stability of the such fixed points become a more subtle topic in this spatiotemporal frame. We will comment on their stability, once we derive the analytical solutions. Again, the system (5) is nonlinear and a straightforward analytical solution is not possible. We therefore define and explore two biological scenarios that allow for an analytical solution under given assumptions. In Scenario 1, we will consider the inhibitor $[I]$ and the inactive pro–form $[P]$ as constant in both space and time, considering a situation where auto–activation is mild or replenishment of the inactive form and inhibitor is fast. In Scenario 2, we will assume that a temporal profile for $[P]$ is given for all times which assumes that protein levels of the inactive pro–form are regulated by other processes than by auto–activation, such as by transcription or degradation. In both scenarios, we can describe the systems dynamics by the reduced model

$$\frac{\partial}{\partial t}c_2 \;=\; d_2\nabla_x^2 c_2 + \alpha c_2. \tag{6}$$

Here

$$\alpha \;=\; k_1 c_1(t, x) - k_4 c_3(t, x) - k_2. \tag{7}$$

To initiate the signalling network (5) appropriate initial conditions have to be chosen. We assume that an initial Akt/mTOR activity is present due to IGF-receptor activation

IC1. **Point–like activation:** By this initial condition, we assume a point-like, activation of Akt/mTOR at a particular spatial location. Local enzyme activities may be spontaneously present at a certain location due to intrinsic noise [6].

IC2. **Receptor activation:** Here we assume an IGF-receptor enriched membrane region which leads to activation of Akt/mTOR.

IC3. **Localised depression of activation:** With this initial condition, we assume that most of the muscle cell surface is covered by activated IGF receptors, while a particular spatial region is deprived of receptors or these receptors are blocked. This blockage may be due to a locally acting antagonist that prevents active receptors or due to the fact that parts of the cell surface is not accessible for activation (due to gap or tight juctions [12]).

IC4. **Arbitrary initiator signal:** This is the most general situation, where we consider an anisotropically distributed expression of IGF receptors at the cell membrane, or, equivalently, spatial fluctuations of IGF-stimulating growth factors. We will exploit the linearity of our approximation scenarios and compose an arbitrary initiator signal by means of Fourier series.

Figure 3 depicts examples of the initial conditions IC1–IC4. In the following sections, we will show the effect of the inhibitor I, for all the initial conditions and scenarios. The absence of the inhibitor, will be represented by $c_3 = 0$ in Equation (7).

4. Scenario 1: High protein turnover or mild enzyme activation

4.1. Scenario definition and solution strategy

We now focus on a scenario where the auto–activation velocity is smaller than the protein reproduction. Accordingly, the strength of auto–activation k_1 is assumed to be low (1a) in comparison to the turnover of both, the pro–form P (1c) and the inhibitor I (1e), whose concentrations are considered to remain constant and are denoted by $\bar{c}_1$ and $\bar{c}_3$, respectively.

Under these conditions, α in (7) becomes

$$\alpha \;=\; k_1\bar{c}_1 - k_4\bar{c}_3 - k_2. \tag{8}$$

We note that the solution to (6) has the form

$$c_2(t,x) = \exp(\alpha t)\, u(t,x). \tag{9}$$

Substituting it into (6), yields

$$\frac{\partial}{\partial t} u(t,x) = d_2 \nabla_x^2 u(t,x), \tag{10}$$

which is the homogeneous heat equation with the initial condition $u(0,x) = g(x)$ in a infinite spatial domain. Using a Green function approach [28], the solutions to the equation above are given by

$$u(t,x) \;=\; \int_{-\infty}^{\infty} g(\xi) G(t,x,\xi) d\xi, \tag{11}$$

where $G(t,x,\xi)$ is a Green function defined as

$$G(t,x,\xi) \;=\; \frac{1}{2\sqrt{\pi dt}} \exp\left(-\frac{(x-\xi)^2}{4dt}\right).$$

In the following, we will use Expression (11) to investigate the response of the reaction network with different initial conditions.

4.2. IC1 - Spontaneous local activation

We assume a localised activation of Akt/mTOR at time point $t = 0$. The initial condition $g(x)$ is represented by

$$g(x) = \delta_\mu,$$

where δ_μ stands for a Dirac pulse in $x = \mu$. Inserting $g(x)$ into (11) leads to

$$u(t,x) \;=\; \frac{1}{2\sqrt{\pi d_2 t}} \exp\left(-\frac{(x-\mu)^2}{4d_2 t}\right).$$

By substituting the expression above in (9), the profile of $c_2(t,x)$ is

$$c_2(t,x) = \frac{1}{2\sqrt{\pi d_2 t}} \exp\left(\alpha t - \frac{(x-\mu)^2}{4d_2 t}\right). \tag{12}$$

Let $\mathcal{N}(\circ)$ be a Gaussian function defined as

$$\mathcal{N}(x-\mu, \sigma^2) = \frac{1}{\sqrt{2\pi\sigma^2}} \exp\left(-\frac{(x-\mu)^2}{2\sigma^2}\right). \tag{13}$$

with μ as maximum and σ as the standard deviation.

With this definition, we can express the spatio–temporal profile for $c_2(t, x)$ in (12) as

$$c_2(t, x) = \exp(\alpha t)\mathcal{N}(x - \mu, 2d_2 t). \tag{14}$$

This expression is a Gaussian curve (Figure 4b upper and Figure 4c upper) which is broadening linearly in time and whose amplitude is given by a time–dependent exponential function. We will restrict α to be negative, non zero values as otherwise the exponential term $\exp(\alpha t)$ would grow without bound. This would not only conflict with biological assumptions that proteins cannot infinitely accumulate, but would also violate our assumptions that the concentration of the activated form is low enough not to decrease the levels of the pro–form of Akt/mTOR or the inhibitor. For the condition $\alpha < 0$, the maximum value for this Gaussian function is found at $x = \mu$; i.e. at the location where the spontaneous activation originally took place. We conclude that a point–like activation of Akt/mTOR will remain localised, but will broaden and decay over time. Figure 4 shows the comparison of the numerical simulation of the model in (5) (Figure 4(a) upper) with the analytical solution with and without inhibitor (Figure 4(b-c) upper, respectively). As we can perceive, the effect of the inhibitor restrains the signals progression in space. By comparison of panels Figure 4(a) upper and Figure 4(b) upper, we note that the behaviour of the approximated Scenario 1, resembles that of the numerical simulation.

4.3. IC2 - Receptor activation

We now study the effect of IFG-receptor activation, by representing initially active Akt/mTOR by a Gaussian distribution as an initial condition ($t = 0$). By this, we assume that receptor activation at the cell membrane extends over a finite spatial region at the cell surface. We define

$$g(x) = k\mathcal{N}(x - \mu, \sigma^2),$$

as initial signal with μ as location of maximum activation and σ as the activation spread. Substitution of this initial condition into (11), leads to

$$\begin{aligned} u(t,x) &= \frac{k}{2\pi\sigma\sqrt{2d_2t}} \\ &\quad \int_{-\infty}^{\infty} k\exp\left(-\left[\frac{\sigma^2(x-\xi)^2+2d_2t(\xi-\mu)^2}{4d_2t\sigma^2}\right]\right)d\xi \\ u(t,x) &= \frac{k}{\sqrt{2\pi(2d_2t+\sigma^2)}}\exp\left(-\frac{(x-\mu)^2}{4d_2t+2\sigma^2}\right). \end{aligned}$$

Substituting this last solution into (9), the spatio–temporal profile for $c_2(t,x)$ gives

$$\begin{aligned} c_2(t,x) &= \frac{k}{\sqrt{\pi(4d_2t+2\sigma^2)}}\exp\left(\alpha t-\frac{(x-\mu)^2}{4d_2t+2\sigma^2}\right) \\ c_2(t,x) &= k\exp(\alpha t)\mathcal{N}(x-\mu,2d_2t+\sigma^2). \end{aligned} \tag{15}$$

We note that Equations (10) and (11) translate an initial Gaussian function into a Gaussian with a maxiumum at the same location (see Figure 4(b–c) lower) whose amplitude is modulated by a time–dependent exponential function. A numerical illustration of a typical solution of this scenario in the presence or absence of an inhibitor is given in the lower panels of Figure 4, where we also compare this approximative scenario to the exact solution of the equation system (5) for a situation where enzyme activation is sufficiently low and protein turnover sufficiently high.

Due to the linearity of (10), any composition of Gaussian functions as initial condition, yields a composition of Gaussian functions. To show this, consider the initial condition

$$g(x)=\sum_{i=1}^{N}k_i\mathcal{N}(x-\mu_i,\sigma_i^2).$$

From (9) it follows that

$$\begin{aligned} u(t,x) &= \int_{-\infty}^{\infty} \left[\sum_{i=1}^{N} k_i \mathcal{N}(x-\mu_i, \sigma_i^2) \right] G(x,\xi,t) d\xi \\ &= \sum_{i=1}^{N} \left[\int_{-\infty}^{\infty} k_i \mathcal{N}(x-\mu_i, \sigma_i^2) G(x,\xi,t) d\xi \right] \\ u(t,x) &= \sum_{i=1}^{N} k_i \mathcal{N}(x-\mu_i, 2d_2 t + \sigma_i^2), \end{aligned}$$

whence,

$$c_2(t,x) = \exp(\alpha t) \sum_{i=1}^{N} k_i \mathcal{N}(x-\mu_i, 2d_2 t + \sigma_i^2). \tag{16}$$

As in the previous case, each Gaussian function will decay exponentially and broaden linearly in time. We conclude that due to the linearity of scenarios 1, receptor activations that happen at different spatial loci linearly superimpose. This will allow us to study arbitray initial conditions (IC4).

4.4. IC3 - Localised depression of activation

We now study the situation where most of the cell surface is covered by activated IGF receptors, while some regions either do not have any receptors, these receptors are blocked or not accessible. For this, assume the initial condition along x at $t = 0$ be represented by the function

$$g(x) = h(x) - h(x-\tau) + h(x-(\tau+\gamma)), \tag{17}$$

where $h(z)$ is the Heaviside step function, defined as

$$h(z) = \begin{cases} 0 & , \quad z < 0 \\ 1 & , \quad z \geq 0. \end{cases}$$

In (17), $0, \tau$ and γ are the spatial locations where the function $g(x)$ suddenly changes its value. According to (9) and (11), the solution in this case is

$$\begin{aligned} u(t,x) &= \frac{1}{2} \left[\operatorname{erf}\left(\frac{x}{2\sqrt{d_2 t}} \right) - \operatorname{erf}\left(\frac{x-\tau}{2\sqrt{d_2 t}} \right) + \right. \\ &\quad \left. + \operatorname{erf}\left(\frac{x-(\tau+\gamma)}{2\sqrt{d_2 t}} \right) + 1 \right]. \end{aligned}$$

Where

$$\mathrm{erf}(z) = \frac{2}{\sqrt{\pi}} \int_0^z \exp(-y^2) dy,$$

and hence,

$$\begin{aligned} c_2(t,x) &= \frac{1}{2}\exp(\alpha t)\left[\mathrm{erf}\left(\frac{x}{2\sqrt{d_2 t}}\right) - \mathrm{erf}\left(\frac{x-\tau}{2\sqrt{d_2 t}}\right) + \right. \\ &\left. + \mathrm{erf}\left(\frac{x-(\tau+\gamma)}{2\sqrt{d_2 t}}\right) + 1\right]. \end{aligned} \tag{18}$$

This solution shows that a discontinuous initial condition (see Figure 3(c)) will eventually 'smoothen' due to the diffusion effect, hence active signals resulting from IGF activation will reach regions in the space in which originally no activated enzyme was present. For high diffusion constant, the activated enzyme may replete all the regions.

4.5. IC4 - Periodic initiator signal.

As demonstrated before, the linearity of (11) allows superimposition of initiator signals. This enables us to study the most general case where IGF receptor activation happens periodically over the entire cell surface. In order to take into account any other 2π–periodic initial condition, we consider we have available the Fourier series of such a signal. Let this representation be given by the infinite series

$$g(x) = \frac{a_0}{2} + \sum_{n=1}^{\infty} \left(a_n \cos(nx) + b_n \sin(nx)\right), \tag{19}$$

where the coefficients a_n and b_n are given by

$$\begin{aligned} a_0 &= \frac{1}{\pi}\int_{-\pi}^{\pi} g(\xi) d\xi \\ a_n &= \frac{1}{\pi}\int_{-\pi}^{\pi} g(\xi)\cos(n\xi) d\xi \\ b_n &= \frac{1}{\pi}\int_{-\pi}^{\pi} g(\xi)\sin(n\xi) d\xi. \end{aligned}$$

Although this series requires the restriction to 2π periodic signals, rescaling of the space variable x allows to include any periodicity of the initial signal $g(x)$.

From (9) and (11) follows,

$$u(t,x) = \frac{a_0}{2} + \sum_{n=1}^{\infty} \exp(-d_2 t n^2) \left(a_n \cos(nx) + b_n \sin(nx)\right),$$

which leads to

$$\begin{aligned} c_2(t,x) &= \frac{a_0}{2} \exp(\alpha t) + \\ &\quad + \sum_{n=1}^{\infty} \exp((\alpha - d_2 n^2)t) \left(a_n \cos(nx) + b_n \sin(nx)\right). \end{aligned} \tag{20}$$

The solution to (11) driven by the initial condition in (19), preserves the original infinite–series form. However, while the exponential damping factor in (20) varies linearly in time, it dependes quadratically on the frequency (n). Consequently, the system (6) acts as a low–pass filter.

4.6. Example for low–pass filtering

We now illustrate how the solution (11) establishes a low–pass filter, that filters out spatial fluctuations in initial IGF receptor mediated signals. We therefore consider the following initial signal as depicted in Figure 5(a)

$$g_1(x) = \frac{1}{2} + 0.3 \sin(x),$$

which is an exemplification of (19) with the Fourier constant $a_0 = 1$ and $b_1 = 0.3$, while other coefficients are zero. According to (20) the solution for this particular initial condition is (Figure 5(d))

$$c_2(t,x) = \frac{1}{2} \exp(\alpha t) + 0.3 \exp((\alpha - d_2)t) \sin(x).$$

Now, consider a different initiator signal composed as the sum of two sine functions (Figure 5(b))

$$g_2(x) = \frac{1}{2} + 0.3 \sin(x) + 0.05 \sin(16x).$$

with the Fourier coefficients for (19) being $a_0 = 1$, $b_1 = 0.3$, $b_{16} = 0.05$ and the remaining coefficients being zero. This initiator signal yields the solution

$$\begin{aligned} c_2(t,x) &= \frac{1}{2} \exp(\alpha t) + 0.3 \exp((\alpha - d_2)t) \sin(x) + \\ &\quad + 0.05 \exp((\alpha - 256 d_2)t) \sin(16x). \end{aligned}$$

From this last equation we see that the term $\exp((\alpha - 256d_2)t)$ approaches zero quickly. Therefore, high harmonics of the initiator signal are filtered out as shown in Figure 5(e). As consequence both initiator signals $g_1(x)$ and $g_2(x)$ will yield a similar spatiotemporal profile $c_2(t_1, x)$ for a sufficient large t_1, regardless of their difference suggesting that reduced system (6) acts as noise repressor.

4.7. Example for spatial fluctuations

Now, consider a 'noisy' Gaussian function as an initial condition, represented as

$$g_2(x) = \mathcal{N}(x - \mu, \sigma^2) + 0.005 \sin(10x) .$$

This initial condition is depicted in Figure 5(c). Due to the linearity of the heat equation, the solution (9) with the foregoing initial condition will be the sum of two terms:

$$c_2(t, x) = \exp(\alpha t)\mathcal{N}(x-\mu, 2d_2t+\sigma^2)+0.005 \exp((\alpha-100d_2)t) \sin(10x). \quad (21)$$

Again, we note that the filtering effect of the heat equation will decrease the spatial fluctuations, since the second element of the sum will decrease in magnitude very quickly as time increases, as noted in the previous example. The solution for $t = t_f = 0.15[s]$ is given in Figure 5(f).

4.8. Summary scenario 1

Table 1 summarises the closed–form expressions for the initial conditions IC1–IC4. All solutions consist of a product of bounded function with an exponential term. As the latter terms determines whether a solution is bounded or not, their arguments must fulfill certain conditions given in Table 2 as otherwise our assumptions of the invariance of $[P]$ and $[I]$ are not anymore fulfilled. Since the exponent $\alpha(t)$ must be negative, no 'on steady state' is present. Likewise, as can be seen from the 1, no travelling wave exists (see remarks regarding travelling waves in section 7.2. The absence of a stable 'on state' and, therefore, of travelling waves is explained by the fact that the assumptions of this scenario (low auto–activation relative to a high protein turnover) violate the assumption $k_2/k_1 < k_{3b}/k_{3f}$. This is consistent with the situation in the space independent scenario, where no 'on state' is observed when the auto–activation kinetic parameter was small compared to protein protein production and degradation (1a).

We conclude this section by noting that our analytical solutions allow exact determination of those times and locations where a certain activation threshold is exceeded (Appendix 7.3) and makes it possible to determine those spatial regions of the muscle cell that may be affected by localised receptor activation. This also allows to assess the effect of inhibitors of the Akt/mTOR pathway such as PTEN that have been implicated in regulating the threshold for Akt/mTOR signalling [11, 25].

5. Scenario 2: Highly regulated protein synthesis

5.1. Scenario definition and solution strategy

In the previous section we have harnessed the linearity of our approximate equation (11) to study IGF receptor signal superposition and arbitrary IGF activation signals. We now aim to provide a generalised scenario (denoted here Scenario 2, yet this is actually a more general case) for that the assumption of linearity remains valid so that the findings of the previous paragraph can be translated into a more general framework. For this general scenario, we assume that the spatial distribution of the pro–enzyme is isotropic and its temporal profile is given *a priori*. This is equivalent to conditions where protein levels are regulated by transcription/translation or by protein degradation rather than by loss and gain through the protein signalling cascades.

Assuming a time–varying stimulus for c_1 and a constant concentration for c_3, we obtain from (7)

$$\alpha \quad = \quad \alpha(t) \quad = \quad k_1 c_1(t) - k_4 \bar{c}_3 - k_2. \tag{22}$$

Accordingly, (6) becomes

$$\frac{\partial}{\partial t} c_2 \;=\; d_2 \nabla_x^2 c_2 + \alpha(t) c_2. \tag{23}$$

In order to write Equation (6) as a homogeneous heat equation we introduce the auxiliary variable $\phi(t)$ that satisfies

$$\dot{\phi}(t) \quad = \quad \alpha(t)\phi(t), \phi(0) = 1, \phi(t) \neq 0 \; \forall \; t \geq 0, . \tag{24}$$

This allows us to define the change of variables from $c_2(t, x)$ to $u(t, x)$ as

$$c_2(t, x) \quad = \quad \phi(t) u(t, x), \tag{25}$$

which leads to the PDE

$$\begin{aligned}\frac{\partial}{\partial t}\{\phi(t)u(t,x)\} &= d_2\nabla_x^2\{\phi(t)u(t,x)\} + \\ &\quad +\alpha(t)\phi(t)u(t,x) \\ \frac{\partial}{\partial t}u(t,x) &= d_2\nabla_x^2 u(t,x).\end{aligned}$$

Expressions (25) and (24) imply that the initial conditions given to $u(t,x)$, are the same initial conditions as those given to $c_2(t,x)$. This can be seen as follows

$$c_2(0,x) = \phi(0)u(0,x) = u(0,x). \tag{26}$$

Consequently, by the transform (26) we have translated the dynamical equation of Scenario 2 to a homogeneous heat equation equivalent to (11) with the same boundary conditions as before. To obtain the respective solutions, we only have to replace the exponential term in Table 1 by the auxiliary variable $\phi(t)$. The respective solutions for the initial conditions IC1 – IC4 are given in Table 3. We note that, since the auxiliary function $\phi(t)$ is only time dependent and since (26) is linear, the dynamical system in this scenario acts also as a low-pass filter for spatial signal fluctuations. Typical auxiliary functions $\phi(t)$ will be given in the next subsection.

5.2. Application to IGF activation during enzyme up and downregulation

Finally, we study activation profiles of active Akt/mTOR for situations where levels of the inactive form are either monotonically up- or downregulated. This regulation is assumed to be caused by processes independent from the auto–activation cascade. This assumption accounts for the presence of intrinsic (non receptor mediated) stress that may enhance or block protein production. As such, activation of the energy sensor AMPK that senses a depletion of cellular ATP (and increase of AMP) has been shown to switch off protein production [30]. Both, AMPK activation and IGF receptor stimulation are simultaneously present during physical exercise and therefore may act in a synergistic fashion. Moreover, cells may also up- or downregulate their Akt/mTOR levels in response to pharmacophores [1].

To model up- and down regulation we set $c_1(t)$ to

$$c_1(t) = k_1^{-1}\left[k_2 + k_4\bar{c}_3 - r + 2\frac{k}{\pi}\arctan(st)\right], \tag{27}$$

where we also assumed a constant inhibitor $\bar{c}_3$. Here, r is a term to adjust the initial value of $c_1(t)$, s is the velocity for attaining a new steady state, while k is the scaling factor that describes the amount of decrease (negative k) or increase (positive k). From (22) we obtain,

$$\alpha(t) = -r + 2\frac{k}{\pi}\arctan(st), \tag{28}$$

which allows us to obtain the auxiliary function $\phi(t)$ by using (24)

$$\begin{aligned}
\ln(\phi(t)) &= \int \alpha(t)dt \\
\ln(\phi(t)) &= -rt + 2\frac{k}{s\pi} \times \\
&\quad \times \left[st\arctan(st) - \ln\left((1+(st)^2)^{\frac{1}{2}}\right)\right] \\
\phi(t) &= \left(1+(st)^2\right)^{-\frac{k}{s\pi}} \exp\left(\alpha(t)t\right), \quad \phi(0) = 1.
\end{aligned} \tag{29}$$

The temporal profile for $c_1(t)$ (see Figure 6a) as described in (27) together with parameter variation of s and k allows us to study $c_2(t,x)$ in response to IGF activation and in response to up- and down regulation of $c_1(t)$. We consider the following situations:

1. **Downregulation of the inactive pro-form:** For modelling downregulation, k needs to be negative and $|k| < [k_2 + k_4\bar{c}_3 - r]$, according to (27) for maintaining positive $c_1(t)$. Note that $c_1(t)$ decreases monotonously. As $\alpha(t)$ is negative, $c_2(t,x)$ decreases exponentially as t increases, although this decrease is slightly attenuated by the first factor. We note two phases of the exponential decay: *i*) for small t, the arcus tangens can approximated by a linear function in t and the second factor leads to an exponential decay quadratic in t. *ii*) For large enough t, the arcus tangens is close to $(\pi/2)$ leading to an exponential decay whose argument is linear in t. Figure 6c shows $c_2(t,x)$ when a localised depression of activation (IC3) is considered, when $c_1(t)$ is being downregulated, as in Figure 6a.
2. **Upregulation of the inactive pro-form:** Here k is positive and $c_1(t)$ increases to a maximum value. Moreover, $\alpha(t) < 0$ needs to be negative as otherwise $c_2(t,x)$ grows without bound. Therefore, protein levels of $c_1(t)$ in (27) must be less than $(k_2 + k_4\bar{c}_3)/k_1$ suggesting that not all

protein productions are biologically possible. Under these conditions, the exponential decay of $c_2(t,x)$ remains dominant. Figure 6b shows $c_2(t,x)$ under IC3 and $c_1(t)$ upregulation.

3. **Reduction to scenario 1:** If k is set to zero, $\alpha(t)$ and c_1 are constant. With negative $\alpha(t) = -r$, the auxiliary function $\phi(t)$ turns into a linearly decaying exponential function and the solution of Scenario 1 are obtained (see Table 1).

Anew, in all above situations, the active Akt/mTOR form $c_2(t)$ decreases with time and, according to Table 1, no travelling waves exist. In conclusion, in Scenario 2 we assumed spatially invariant, but temporarily variant protein profiles of the pro–form that are imposed by other processes than receptor activation, such as energy stress. We found that assuming such profiles did not change the fact that spatial fluctuations in IGF receptor activation are filtered out, resulting in a more homogeneous Akt/mTOR activation.

6. Summary and Discussion

In this study, we provided an analytical approach to investigate signal transduction in time and space in large, but thin cells mediated by a simple auto–activation loop and a receptor stimulus. By applying our approach to growth (changes in diameter) in skeletal muscle cells, we have gained insights into the question under what circumstances a stable activation of AKT/mTOR can be achieved and how spatial anisotropies may be translated into a homogeneous response along the entire cell. We first focussed on time dependent, but spatially invariant signal propagation and determined conditions for a stable AKT/mTOR activation. These conditions required the strength of auto-feedback to be high compared to protein turnover.

We investigated spatiotemporal signal propagation assuming four different initiator signals that describe IGF receptor activation. To solve them analytically, we have developed biologically justified scenarios. We first considered a scenario where protein turnover was faster compared to enzyme auto–activation. The distribution of the active enzyme was found to broaden in space (yet staying localised) and its magnitude was decaying exponentially over time. Unlike in a general scenario, where a stable 'on state' and travelling waves may exist, no such state and no travelling waves were found under our scenario assumptions. Our results therefore suggest that high protein turnover may 'wash out' the active pro–form, keeping it locally confined to

the place where they originated from (e.g. IGF receptor). Indeed, there are evidences in literature where enzymes that lead to a more severe response such as cell–cycle arrest or cell death when they act over the entire cell, have a distinctive, physiological role when they are spatially and temporally localised [36]. As an example, proteases that mediate cell death in other large cells such as nerve cells are essential for the physiological process of long–term potentiation when their activity remains localised at the nerve cells' synapses [20].

Changes in protein turnover may therefore mediate between a localised physiological and a global detrimental role of the same enzyme.

In scenario 2, we assumed to know the amount of pro–enzyme that is available at a given time. This is equivalent to study signal progression under variation of protein production. Such variations may arise from physiological or pharmacologic inhibition of protein production or, in contrast, from elevation of protein production induced by trophic factor stimulation or pharmacologic treatments [4, 8, 13, 27]. Also under these assumptions, no stable 'on state' and no travelling waves were identified.

For both approximation scenarios, the dynamics of the active form was governed by a homogeneous heat equation and therefore by a linear PDE. Thus, studying these scenarios analytically, we were able to superimpose solutions and represent a general receptor activation by Fourier series. While the exponent responsible for damping the Gaussian pulses was found to be linear in time, it was a quadratic function of the frequency of the harmonics that compose the original signal. As consequence, the contribution of harmonics with higher frequencies approach zero faster. By this, auto–activation together with diffusion can act as low–pass filters. This filter can translate spatial fluctuations arising from spatial heterogeneity in IGF activation into a more uniform distribution of enzyme activation.

In conclusion, our study highlights the importance of studying spatiotemporal signal transduction in large cells by rigorous mathematical methods and helped to elucidate how receptor mediated signals can propagate or can get attenuated, and how spatial fluctuations of receptor activation can be filtered. While our study was motivated by mTOR/AKT kinase signalling networks, the results can be applied to a variety of cases such as MAPK signalling during cell proliferation [32], protease cascades during cell death [16], and the establishment of cell polarity by morphogens during development [5] in any large cell or cell compartment.

7. Appendix

7.1. Autoactivation of Akt

In this section, we show how the mTOR/Akt interaction leads to an Akt autoactivation, when the mTOR levels can be considered constant. This can happen *i*) under the presence of a big pool of mTOR in comparison to the Akt pool, or *ii*) the mTOR concentration is kept constant due to high a turnover rate.

In order to reduce the pathway, we will consider that the extracellular stimulus of insulin is translated via the IGF receptor into an initial condition of phosphorilised Akt (Akt_a). The inactive version of Akt (Akt) can also be activated by its interaction with $mTOR$. Here $mTOR$ represents the mTOR complex under physiological conditions, which we assume to keep a constant concentration due to high turnover rates, or due to the abundance of $mTOR$ so the Akt/mTOR interaction does not deplete the $mTOR$ pool, significantly. Also, Akt_a is further deactivated and degraded. Moreover, we will include the effect of an inhibitor of Akt_a, which will be denoted by I. Finally, both Akt and I will be endowed with a synthesis and degradation. These interactions and effects are summarised by the forthcoming reactions:

$$Akt_a \xrightarrow{\tilde{k}_0} mTOR + Akt_a \tag{30a}$$

$$Akt + mTOR \xrightarrow{\tilde{k}_1} Akt_a + mTOR \tag{30b}$$

$$Akt_a \xrightarrow{k_2} 0 \tag{30c}$$

$$Akt \underset{k_{3b}}{\overset{k_{3f}}{\rightleftharpoons}} 0 \tag{30d}$$

$$Akt_a + I \xrightarrow{k_4} 0 \tag{30e}$$

$$I \underset{k_{5b}}{\overset{k_{5f}}{\rightleftharpoons}} 0 \tag{30f}$$

Writing one after another the reactions (30a) and (30b), we have

$$Akt + Akt_a \xrightarrow{\tilde{k}_0} mTOR + Akt_a + Akt \xrightarrow{\tilde{k}_1} 2Akt_a + mTOR. \tag{31}$$

Note that we have added Akt as a product and a reactant to the first reaction without assuming it to have an impact on the reaction rate k_0. This was done

to include Akt as a reactant for the second reaction in (31). Now, if $\tilde{k}_0 >> \tilde{k}_1$, we can reduce the reaction (31) to

$$mTOR + Akt_a + Akt \xrightarrow{\tilde{k}_1} 2Akt_a + mTOR \tag{32}$$

or more compactly, as

$$Akt + Akt_a \xrightarrow{mTOR \times \tilde{k}_1} 2Akt_a \tag{33}$$

By choosing $P = Akt$, $A = Akt_a$, and $k_1 = mTOR \times \tilde{k}_1$; we can express the network in (30) as

$$\begin{aligned} P + A &\xrightarrow{k_1} 2A \\ A &\xrightarrow{k_2} 0 \\ P &\underset{k_{3b}}{\overset{k_{3f}}{\rightleftharpoons}} 0 \\ A + I &\xrightarrow{k_4} 0 \\ I &\underset{k_{5b}}{\overset{k_{5f}}{\rightleftharpoons}} 0. \end{aligned}$$

Note that this is the same reaction network as presented in (1).

7.2. Travelling waves

Travelling waves are fronts of active enzymes that propagate along space and time with a constant shape. Although their presence can be easily shown numerically, analytical proofs of their existence remain cumbersome. We here refer to an existence proof that applies to a restricted scenario. In this scenario, we only consider the auto–activation reaction (1a) and assume at the same time that the sum of concentrations of the active and the inactive form remains conserved, $Z = P + A = \text{const}$. This assumes that production of the inactive form, generation of the active form by auto–activation and degradation of the active form are well balanced. We note that, in contrast to our scenarios in the main text, this assumption does not require protein production to be fast or auto–activation to be slow. The dynamic equation for the concentration of the active enzyme $[A]$ takes the form

$$\frac{\partial}{\partial t}[A] = d_2 \nabla_x^2 [A] + k_1 [A]([Z] - [A]). \tag{34}$$

Assuming proper scaling units, we consider the concentration of the total protein to be normalised, $[Z] = 1$. Equation (34) is then known as the Fisher–Kolmorov equation, which was first proposed by Fisher [10] and later studied by Kolmogorov [19]. Conditions for the existence of travelling waves were derived in [10] and reviewed in [24], Chap. 13, where we refer the reader for details. These conditions indicate that wave speed should be greater than $2(k1D)^{1/2}$ in order to obtain a phase portrait with a heterocyclic curve connecting the saddle point with the stable node in the equivalent set of ODE derived from the PDE. Under these circumstances, the solution of the PDE system will evolve to a travelling wavefront whenever the initial conditions are a step function for receptor activation, i.e.

$$[A](x,0) = \begin{cases} 1 & \text{if } x \leq x_1 \\ 0 & \text{if } x \geq x_2. \end{cases}$$

with $x_1 < x_2$ and $x_1 < x < x_2$.

We finally remark that taking into account arbitrary protein production and degradation as in the full dynamic system (1) requires an analysis that accounts for variations of Z over time.

7.3. Investigating thresholds from analytical solutions

In this section, we discuss how the availability of analytical solution can help to determine those spatial regions of a muscle cell where the Akt/mTOR activation exceeds a certain threshold. Indeed, Akt and mTOR have been shown to exert their role as a growth signal only when certain thresholds are reached. The Akt/mTOR antagonist PTEN has been shown to regulate these thresholds [11, 25]. We will further motivate how threshold determination from analytical solutions may aide in determining the applicability of mass action kinetics in our scenario. We will focus here on the closed formulas for the active form $c_2(t,x)$ that were obtained in the receptor activation scenario IC2 (15) in Section 4. Assumings a threshold ($\tilde{c}_2$) for c_2, we obtain

$$\tilde{c}_2 \quad \leq \quad \frac{k}{\sqrt{\pi(4d_2t + 2\sigma^2)}} \exp\left(\alpha t - \frac{(x-\mu)^2}{4d_2t + 2\sigma^2}\right).$$

From above equation, we can obtain the area around the original centre of activation μ where the threshold is exceeded at a certain time t

$$|x-\mu| \leq \sqrt{(4d_2t+2\sigma^2)\left[\alpha t - \frac{1}{2}\ln\left(k^{-2}\tilde{c}_2^2\pi(4d_2t+2\sigma^2)\right)\right]}. \tag{35}$$

We recall that the dynamical system (1) was modelled by mass–action kinetics. Consequently, Equation (35) may serve to evaluate whether or not the conditions of mass action kinetics (sufficiently high values of c_1 and c_2) are fulfilled and whether or not c_2 is reliable in this area. Otherwise stochastic effects have to be taken into account. We further note that valid thresholds $\bar{c}_2$ require the argument of the square root to be positive and therefore Equation (35) allows to validate whether a threshold is reached or not. Comparing spatial patterns of exceeded thresholds (35) to experiments that measure the result of mTOR/AKT activation (such as spatial regions of muscle growth), may therefore give insights into the quantitative kinetics (k, d_2) of Akt/mTOR activation and into the kinetics of Akt/mTOR inhibition by PTEN. Finally, we remark that the diffusion constant has a direct relationship to the size of the area exceeding the threshold, whereas the inhibitor tends to confine the signal to its original location. An example of threshold determination over space is given in Figure 7.

Acknowledgments

F. L–C. acknowledges the support of Dr D. Kalamatianos. This work was supported through the National Biophotonics and Imaging Platform, Ireland, and funded by the Irish Government's Programme for Research in Third Level Institutions, Cycle 4, Irelands EU Structural Funds Programmes 2007–2013.
R. H. M & M. R. G acknowledge the support by Science Foundation Ireland via grant 07/IN.1/I1838.
H. J. H. acknowledges the support by Science Foundation Ireland via grant 08/IN.1/B1949.

References

[1] Amaravadi, R., Oct. 2005. The survival kinases akt and pim as potential pharmacological targets. Journal of Clinical Investigation 115, 2618–2624.

[2] Bird, R. B., Stewart, W. E., Lightfoot, E. N., 2006. Transport Phenomena, 2nd Edition. Wiley.

[3] Bodine, S. C., Stitt, T. N., Gonzalez, M., Kline, W. O., Stover, G. L., Bauerlein, R., Zlotchenko, E., Scrimgeour, A., Lawrence, J. C., Glass, D. J., Yancopoulos, G. D., Nov. 2001. Akt/mTOR pathway is a crucial regulator of skeletal muscle hypertrophy and can prevent muscle atrophy in vivo. Nature Cell Biology 3 (11), 1014–1019, PMID: 11715023.

[4] Bolster, D. R., Crozier, S. J., Kimball, S. R., Jefferson, L. S., 2002. Amp-activated protein kinase suppresses protein synthesis in rat skeletal muscle through down-regulated mammalian target of rapamycin (mtor) signaling. Journal of Biological Chemistry 277 (27), 23977–23980.

[5] Davidson, E., 1991. Spatial mechanisms of gene regulation in metazoan embryos. Development 113 (1), 1–26.

[6] Eissing, T., Allgoewer, F., Bullinger, E., 2005. Robustness properties of apoptosis models with respect to parameter variations and intrinsic noise. IEE Proceedings - Systems Biology 152, 221.

[7] Eissing, T., Conzelmann, H., Gilles, E. D., Allgower, F., Bullinger, E., Scheurich, P., 2004. Bistability Analyses of a Caspase Activation Model for Receptor-induced Apoptosis. J. Biol. Chem. 279 (35), 36892–36897.

[8] Ennis, H. L., Lubin, M., 1964. Cycloheximide: Aspects of inhibition of protein synthesis in mammalian cells. Science 146 (3650), 1474–1476.

[9] Ferrell, James E, J., Apr. 2002. Self-perpetuating states in signal transduction: positive feedback, double-negative feedback and bistability. Current Opinion in Cell Biology 14 (2), 140–148, PMID: 11891111.

[10] Fisher, R. A., Jun. 1937. The wave of advance of advantageous genes. Annals of Human Genetics 7 (4), 355–369.

[11] Franke, T. F., Hornik, C. P., Segev, L., Shostak, G. A., Sugimoto, C., ???? PI3K//Akt and apoptosis: size matters. Oncogene 22 (56), 8983–8998.

[12] Friend, D. S., Gilula, N. B., Jun. 1972. Variations in tight and gap junctions in mammalian tissues. The Journal of Cell Biology 53 (3), 758 –776.

[13] Fujii, D., Massoglia, S., Savion, N., Gospodarowicz, D., 1982. Neurite outgrowth and protein synthesis by pc12 cells as a function of substratum and nerve growth factor. The Journal of Neuroscience 2 (8), 1157–1175.

[14] Grant, M., Wargovich, T., Ellis, E., Tarnuzzer, R., Caballero, S., Estes, K., Rossing, M., Spoerri, P., Pepine, C., Dec. 1996. Expression of IGF-I, IGF-I receptor and IGF binding proteins -1, -2, -3, -4 and -5 in human atherectomy specimens. Regulatory Peptides 67 (3), 137–144.

[15] Granville, C. A., Memmott, R. M., Gills, J. J., Dennis, P. A., 2006. Handicapping the race to develop inhibitors of the phosphoinositide 3-kinase/akt/mammalian target of rapamycin pathway. Clinical Cancer Research 12 (3), 679–689.

[16] Huber, H. J., Laussmann, M. A., Prehn, J. H., Rehm, M., 2010. Diffusion is capable of translating anisotropic apoptosis initiation into a homogeneous execution of cell death. BMC Systems Biology 4 (9).

[17] Kaiser, U., Schardt, C., Brandscheidt, D., Wollmer, E., Havemann, K., Nov. 1993. Expression of insulin-like growth factor receptors i and II in normal human lung and in lung cancer. Journal of Cancer Research and Clinical Oncology 119, 665–668.

[18] Klipp, E., Kowald, A., Wierling, C., Lehrach, H., 2005. Systems Biology in Practice: Concepts, Implementation and Application. Wiley-VCH.

[19] Kolmogorov, A., Petrovsky, I., Piskunov, 1937. Etude de léquation de la diffusion avec croissance de la quantité de matiere et son applicationa un probleme biologique. Mosc. Univ. Bull. Math 1, 1–25.

[20] Kuranaga, E., 2011. Caspase signaling in animal development. Development, Growth and Differentiation 53 (2), 137–148.

[21] Kuroda, S., Schweighofer, N., Kawato, M., 2001. Exploration of signal transduction pathways in cerebellar long-term depression by kinetic simulation. The Journal of Neuroscience 21 (15), 5693–5702.

[22] Li, J., Yen, C., Liaw, D., Podsypanina, K., Bose, S., Wang, S. I., Puc, J., Miliaresis, C., Rodgers, L., McCombie, R., Bigner, S. H., Giovanella, B. C., Ittmann, M., Tycko, B., Hibshoosh, H., Wigler, M. H., Parsons, R., Mar. 1997. PTEN, a putative protein tyrosine phosphatase gene mutated in human brain, breast, and prostate cancer. Science 275 (5308), 1943 –1947.

[23] Manning, B. D., Cantley, L. C., Jun. 2007. AKT/PKB signaling: Navigating downstream. Cell 129 (7), 1261–1274.

[24] Murray, J. D., 2002. Mathematical biology: An introduction. Springer.

[25] Ogg, S., Ruvkun, G., Dec. 1998. The c. elegans PTEN homolog, DAF-18, acts in the insulin receptor-like metabolic signaling pathway. Molecular Cell 2 (6), 887–893.

[26] Pallafacchina, G., Calabria, E., Serrano, A. L., Kalhovde, J. M., Schiaffino, S., Jul. 2002. A protein kinase b-dependent and rapamycin-sensitive pathway controls skeletal muscle growth but not fiber type specification. Proceedings of the National Academy of Sciences 99 (14), 9213 –9218.

[27] Peterson, A. L., Nutt, J. G., 2008. Treatment of parkinson's disease with trophic factors. Neurotherapeutics 5 (2), 270 – 280, movement Disorders.

[28] Polyanin, A. D., 2001. Handbook of Linear Partial Differential Equations for Engineers and Scientists, 1st Edition. Chapman and Hall/CRC.

[29] Rommel, C., Bodine, S. C., Clarke, B. A., Rossman, R., Nunez, L., Stitt, T. N., Yancopoulos, G. D., Glass, D. J., Nov. 2001. Mediation of IGF-1-induced skeletal myotube hypertrophy by PI(3)K/Akt/mTOR and PI(3)K/Akt/GSK3 pathways. Nature Cell Biology 3 (11), 1009–1013, PMID: 11715022.

[30] Ruderman, N. B., Park, H., Kaushik, V. K., Dean, D., Constant, S., Prentki, M., Saha, A. K., Aug. 2003. AMPK as a metabolic switch in

rat muscle, liver and adipose tissue after exercise. Acta Physiologica Scandinavica 178 (4), 435–442, PMID: 12864749.

[31] Sarbassov, D. D., Guertin, D. A., Ali, S. M., Sabatini, D. M., 2005. Phosphorylation and regulation of akt/pkb by the rictor-mtor complex. Science 307 (5712), 1098–1101.

[32] Takahashi, K., Tănase-Nicola, S., ten Wolde, P. R., 2010. Spatio-temporal correlations can drastically change the response of a mapk pathway. Proceedings of the National Academy of Sciences 107 (6), 2473–2478.

[33] Tanaka, K., Augustine, G. J., 2008. A positive feedback signal transduction loop determines timing of cerebellar long-term depression. Neuron 59 (4), 608 – 620.

[34] Taylor, V., Wong, M., Brandts, C., Reilly, L., Dean, N. M., Cowsert, L. M., Moodie, S., Stokoe, D., 2000. 5' phospholipid phosphatase ship-2 causes protein kinase b inactivation and cell cycle arrest in glioblastoma cells. Molecular and Cellular Biology 20 (18), 6860–6871.

[35] Wilkins, A., Chandran, S., Compston, A., Oct. 2001. A role for oligodendrocytederived IGF1 in trophic support of cortical neurons. Glia 36 (1), 48–57.

[36] Williams, D. W., Kondo, S., Krzyzanowska, A., Hiromi, Y., Truman, J. W., 2006. Local caspase activity directs engulfment of dendrites during pruning. Nature Neuroscience 9 (10), 1234–1236.

Table 1: Spatio–temporal evolution for the mild enzyme activation scenario (Scenario 1) under different initial conditions

Initial Condition	**Spatio–temporal behaviour** ($c_2(t,x)$)
Point–like activation	$\exp(\alpha t)\mathcal{N}(x-\mu, 2d_2t)$
Receptor activation	$\exp(\alpha t)\sum_{i=1}^{N} k_i\mathcal{N}(x-\mu_i, 2d_2t+\sigma_i^2)$
Localised depression of activation	$\frac{1}{2}\exp(\alpha t)\left[\text{erf}\left(\frac{x}{2\sqrt{d_2t}}\right) - \text{erf}\left(\frac{x-\tau}{2\sqrt{d_2t}}\right) + \text{erf}\left(\frac{x-(\tau+\gamma)}{2\sqrt{d_2t}}\right) + 1\right]$
Arbitrary periodic signal	$\frac{a_0}{2}\exp(\alpha t) + \sum_{n=0}^{\infty}\exp((\alpha - d_2n^2)t)\times (a_n\cos(nx) + b_n\sin(nx))$

Table 2: Conditions for the stability of the solutions to Equation (6) for Scenario 1 and different initial conditions

Initial Condition	**Stability condition**
Point–like activation	$\bar{c}_1 < \frac{k_2+k_4\bar{c}_3}{k_1} + \frac{x^2}{4k_1d_2t^2}$
Receptor activation	$\bar{c}_1 < \frac{k_2+k_4\bar{c}_3}{k_1} + \frac{x^2}{k_1(4d_2t+2\sigma^2)t}$
Localised depression of activation	$\bar{c}_1 < \frac{k_2+k_4\bar{c}_3}{k_1}$
Arbitrary periodic signal	$\bar{c}_1 < \frac{k_2+k_4\bar{c}_3}{k_1}$

Table 3: Spatio–temporal evolution for the stress–induced enzyme activation scenario (Scenario 2) under different initial conditions. Where $\alpha(t)$ and $\phi(t)$ are defined in (28) and (29), respectively.

Initial Condition	**Spatio–temporal behaviour** ($c_2(t,x)$)
Point–like activation	$\phi(t)\mathcal{N}(x-\mu, 2d_2t)$
Receptor activation	$\phi(t)\sum_{i=1}^{N} k_i\mathcal{N}(x-\mu_i, 2d_2t+\sigma_i^2)$
Localised depression of activation	$\frac{1}{2}\phi(t)\left[\text{erf}\left(\frac{x}{2\sqrt{d_2t}}\right) - \text{erf}\left(\frac{x-\tau}{2\sqrt{d_2t}}\right) + \text{erf}\left(\frac{x-(\tau+\gamma)}{2\sqrt{d_2t}}\right) + 1\right]$
Arbitrary periodic signal	$\frac{a_0}{2}\phi(t) + \sum_{n=0}^{\infty}\phi(t)\exp(-d_2n^2t)\times (a_n\cos(nx) + b_n\sin(nx))$

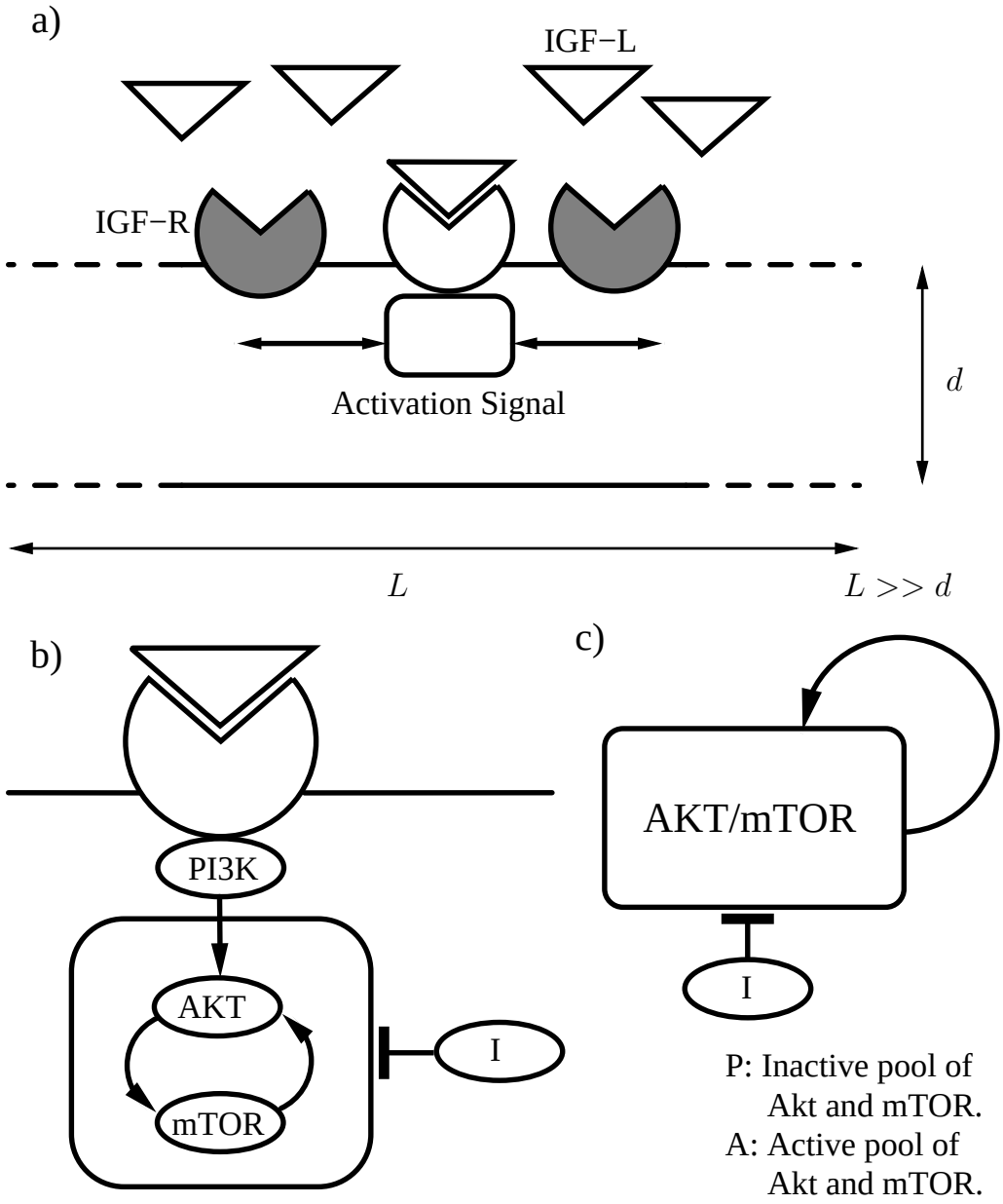

Figure 1: AKT/mTOR pathway activation by IGF stimulation. The panel (a) shows a spatially extended cell ($L >> d$), with IGF receptors (IGF-R) that are activated by binding of IGF ligands (IGF-L). Upon binding, the active signal that originates at the receptor propagates through the cell. The diameter d of the cell is neglected. The behaviour of the active signal at each spatial location is analysed in the main text. Panel (b) details how the receptors activation results in PI3 kinase activation and a subsequent positive feedback loop of Akt and mTOR. Moreover, the effect of an inhibitor I of such a pathway is considered. Panel (c) illustrates the abstraction of Akt and mTOR into one simple node which auto–activates itself as considered in this study. This auto–feedback is assumed to convert inactive versions of Akt/mTOR (P) to their respective active forms (A).

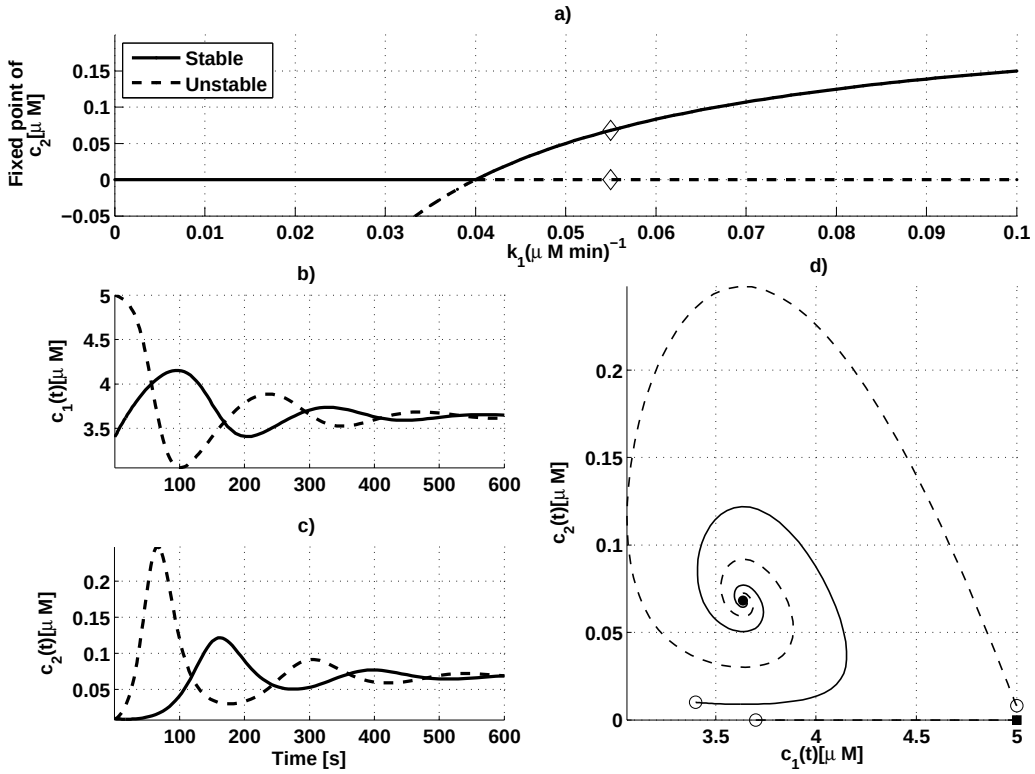

Figure 2: Trajectories and phase portrait due to two different initial conditions for the system in (3). Panel (a) shows the fixed point *loci* of the active enzyme A concentration ($\bar{c}_2$) due to variation on the feedback strength (k_1). In turn, Panel (b) and (c) depict $c_1(t)$ and $c_2(t)$, respectively. Finally, d) shows a phase portrait where we plot the active form $c_2(t)$ vs the inactive form $c_1(t)$. The dot (square) represents (un–)stable steady state and the circles, the initial conditions for each orbit. We see that all the orbits converge to the stable fixed point, except for those whose $c_2(0, x)$ coordinate is zero. This indicates that unstable steady state is a saddle point; in turn, the stable steady state is a focus. Parameters $\{k_1, k_2, k_{3f}, k_{3b}\} = \{0.055, 0.2, 0.01, 0.05\}[(\mu Ms)^{-1}]$.

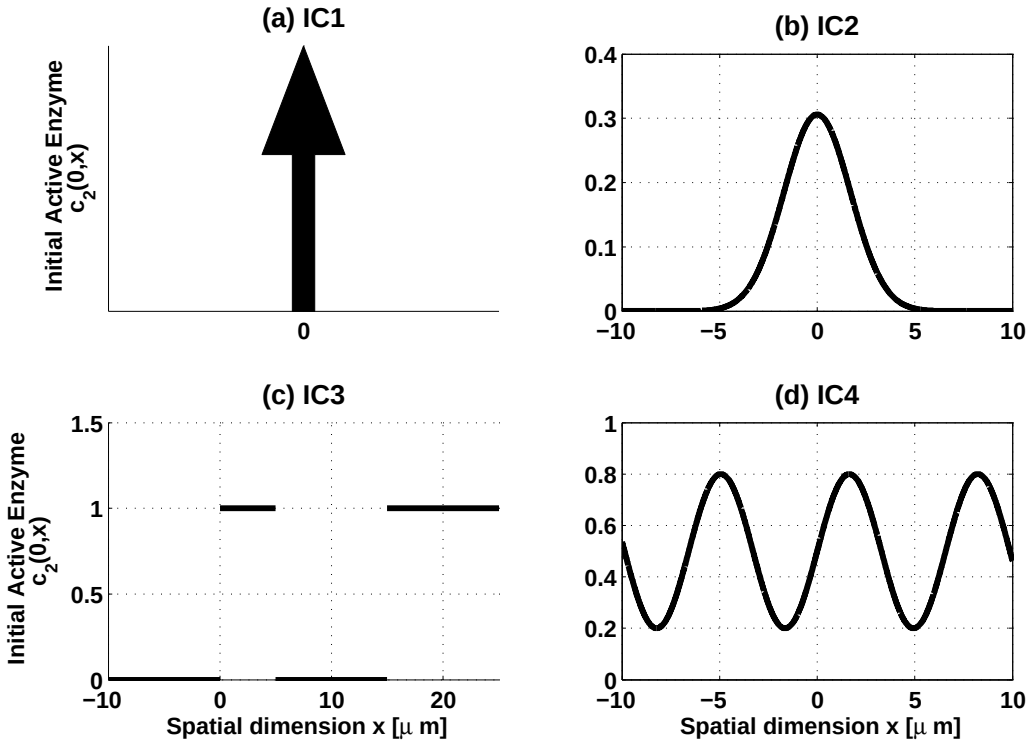

Figure 3: Illustration of typical initial conditions IC1–IC4 as described in Section 4: (a) Dirac delta pulse in the origin, (b) Gaussian curve, (c) a composition of steps, (d) a typical periodic signal.

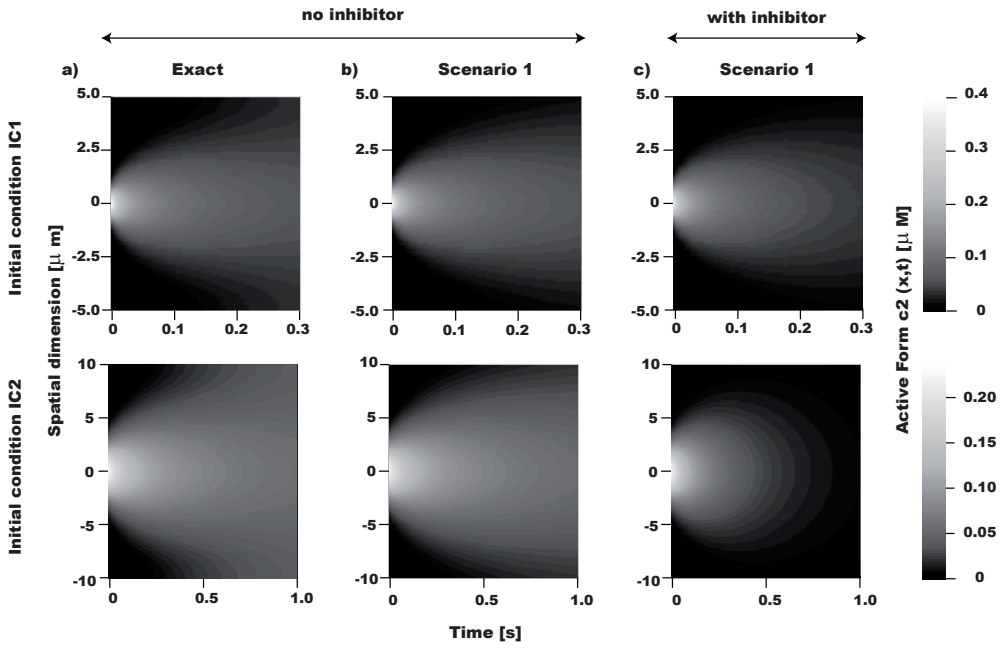

Figure 4: Numerical solution of the exact solution for $c_2(t,x)$ in Eq. (5) (panels (a)) and the approximated Scenario 1 (Eq. (6)) with and without inhibitor (panels (b) and (c), respectively). The upper panels, show the spatiotemporal profile for $c_2(t,x)$ with a the point like activation as initial condition (IC1). In turn, the lower panels, shows $c_2(t,x)$ for a receptor activation (IC2). The presence (absence) of the inhibitor in the columns (b) and (c), is represented by $\bar{c}_3 = 0\,(10)[\mu M]$. In conclusion, the similarity of results in column (a) and (b) illustrate Scenario 1 as a valid approximation when protein turnover is high compared to strength of auto–activation. Parameters $\{k_1, k_2, k_{3f}, k_{3b}, k_4\} = \{k_2/5, 0.2, 0.01, 0.05\}[(\mu M s)^{-1}]$, $k_{in} = 0.5$, $d_2 = 24[\mu m^2/s]$, $\sigma = 1.7$.

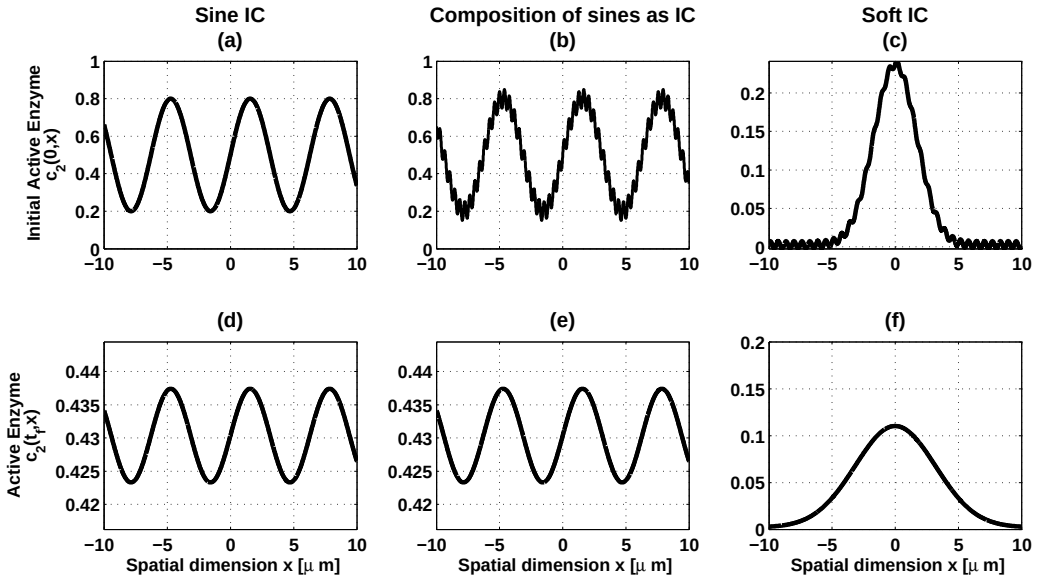

Figure 5: Initial conditions and the solution of Scenario 1 (Eq. (6)), under such initial conditions. The panel (a) depicts a sinusoidal signal of a single frequency; in turn, panel (b) shows a sum of low and high frequency sine functions; finally, panel (c) shows a 'noisy' Gaussian function with $\mu = 0$ and $\sigma^2 = 1.7$. The panels (d–f) depict the solution to (6) at $t = t_f = 0.15[s]$ for the initial conditions (a–c), respectively. We note that in the case of noisy signals, the effect of the noise vanishes, as the time proceeds. Parameters: $\alpha = -1$. Kinetic and diffusion parameters are as in Figure 4.

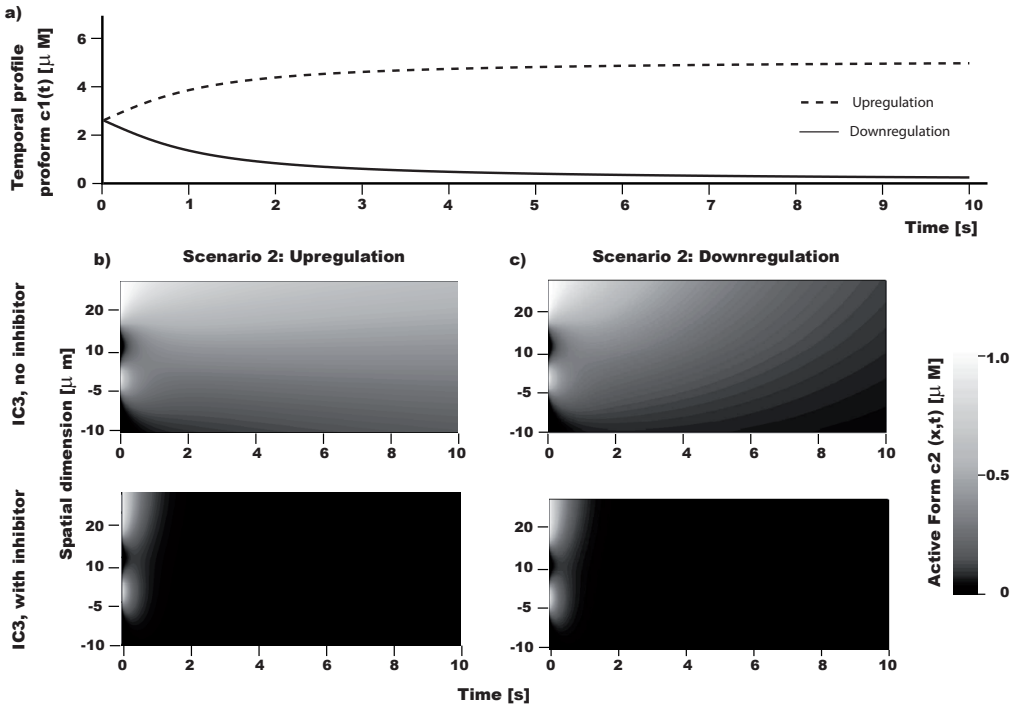

Figure 6: Solution of Scenario 2 (Eq. (6)) under the initial condition IC3 (localised depression of activation). a) Represents up- and downregulation (dashed and dotted line, respectively) of $c_1(t)$ according to cases 1 and 2 in Section 5.2 and given by (27). The panels (b) and (c) show $c_2(t, x)$ when $c_1(t)$ is being upregulated and downregulated, respectively, as shown in panel (a). Furthermore, the upper and lower panels of (b) and (c) present $c_2(t, x)$ with and without inhibitor. We note that the effect of the upregualtion of $c_1(t)$ is a more steady signal progression. Parameters $\tau = 5$, and $\gamma = 15$, $s = 1$. Upregulation: $\{r, k\} = \{0.1, 0.1\}$. Downregulation: $\{r, k\} = \{0.1, -0.1\}$. The rest of the parameters are as in Figure 4.

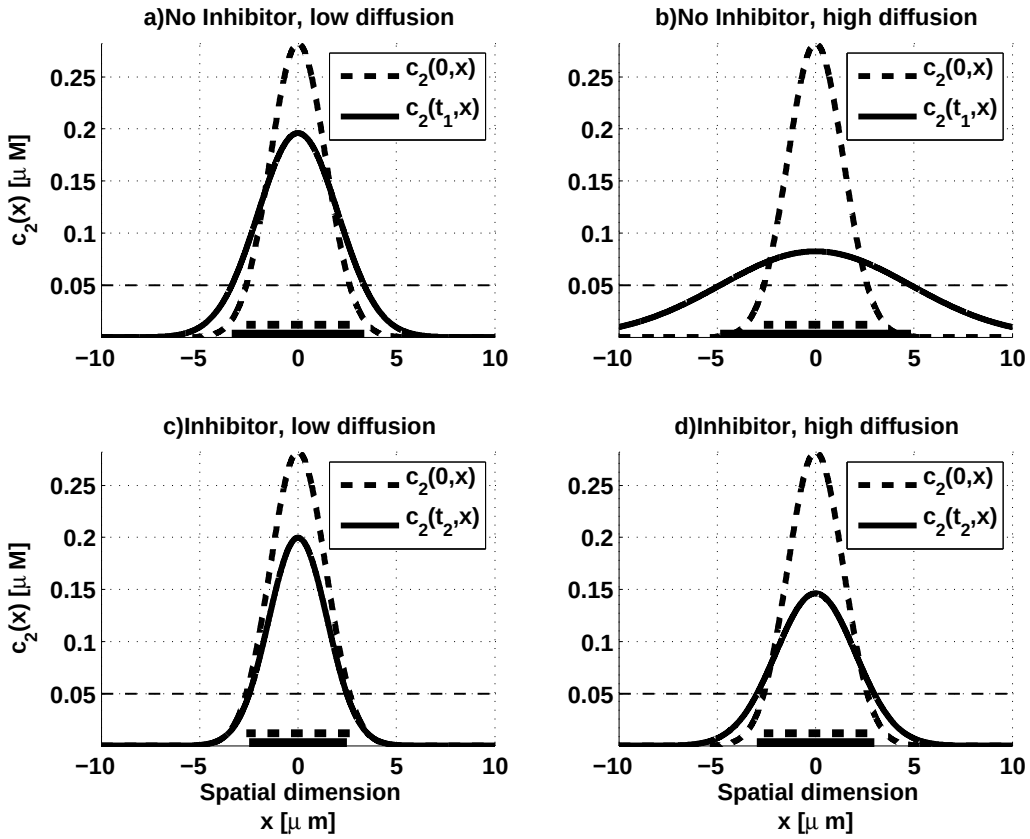

Figure 7: Example of detecting spatial regions in which a concentration threshold (horizontal dotted line) is exceeded. For Scenario 1, we consider a Gaussian initial condition (depicted in a dotted line) with $\mu = 0$ and $\sigma^2 = 1.7$. The panel a) shows the behaviour of the active form $c_2(t_1, x)$ in the absence of inhibitor and with low diffusivity (d_l); in turn, b) depicts $c_2(t_1, x)$ without inhibitor, but with a higher diffusion constant (d_h). Accordingly, c) and d) represent $c_2(t_2, x)$ in the presence of inhibitor with low and high diffusion constants, respectively. The times t_1 and t_2, have been chosen close to the time in which the maximal signal propagation is observed. As we can see, an increase in the diffusion constant or the presence of an inhibitor lead to a decrease in the signals spatial spread. All the curves have been obtained from the formulas in Table 1. Parameters: $\{k_1, k_2, k_4\} = \{0.04, 0.2, 8.3\}[(\mu M min)^{-1}]$; $\{d_l, d_h\} = \{30, 300\}[\mu m^2/min]$; $\{\sigma^2, \mu\} = \{2, 0\}$; $\{\bar{c}_1, \bar{c}_3\} = \{5, 10\}[\mu M]$; $\{t_1, t_2\} = \{0.0357, 0.0035\}[min]$.